



# ALMA-IMF: ALMA transforms our view of the origin of stellar masses

2017.1.01355.L

## ABSTRACT

Studying massive protoclusters is an absolute requirement for investigating the origin of the IMF in the typical, yet extreme environments where massive stars are born.

Recent ALMA imaging of a young massive protocluster revealed the first definitive case of a core mass function (CMF) whose shape is different from the IMF. In contrast, the CMF shape in more evolved but still embedded massive clusters more closely resembles the IMF. This raises the intriguing possibility of CMF evolution with time. We aim to determine when and by which physical processes the CMF of massive protoclusters is reconciled with the canonical IMF.

We propose to investigate the CMF evolution of massive protoclusters with the 15 most massive pc<sup>2</sup> clouds at  $d < 6$  kpc. We will focus on 1) investigating the distribution of 0.5-200 Msun cores at 1-mm and 3-mm at the 2000-AU core size; 2) characterizing the core mass evolution through gas inflows toward individual cores and gas outflows driven by protostars; and 3) compare massive protocluster CMFs to the IMF and determine which variables (such as inflows, outflows, or forming filaments) might be correlated with CMF evolution toward the IMF shape.

<b>PI NAME:</b>	Frederique Motte			<b>SCIENCE CATEGORY:</b>	ISM, star formation and astrochemistry
<b>PI E-MAIL:</b>	frederique.motte@univ-grenoble-alpes.fr			<b>PI INSTITUTE:</b>	IPAG, Institut de Planetologie et d'Astrophysique de Grenoble
<b>ESTIMATED 12M TIME:</b>	<b>63.5 h</b>	<b>ESTIMATED ACA TIME:</b>	<b>296.8 h</b>	<b>ESTIMATED NON-STANDARD MODE TIME (12-M):</b>	<b>0.0 h</b>
<b>CO-PI NAME(S): (Large &amp; VLBI Proposals only)</b>	Adam Ginsburg; Patricio Sanhueza; Fabien Louvet				
<b>CO-INVESTIGATOR NAME(S):</b>	Sylvain Bontemps; Timea Csengeri; Fabrice Herpin; Jordan Molet; Andres Ernesto Guzman; John Bally; Cara Battersby; Brian Svoboda; James Di Francesco; Roberto Galvan-Madrid; Leonardo Bronfman; Quang Nguyen Luong; Fumitaka Nakamura; Thomas Nony; Ana López-Sepulcre; Bilal Ladjelate; Kenneth Marsh; Antoine Gusdorf; Patrick Hennebelle; Jonathan Braine; Satoshi Ohashi; Ken'ichi Tatematsu; Takeshi Sakai; Xing Lu; Vivien Chen; Nicolas Reyes; Ricardo Finger; Karl Menten; Erik Rosolowsky; Gilberto Gomez				
<b>DUPLICATE OBSERVATION JUSTIFICATION:</b>					

## REPRESENTATIVE SCIENCE GOALS (UP TO FIRST 30)

SCIENCE GOAL	POSITION	BAND	ANG.RES.(")	LAS.(")	ACA?	NON-STANDARD MODE
W51-E_3mm	ICRS 19:23:44.1800, 14:30:29.500	3	0.370	80.000	Y	N
W43-MM2_1mm	ICRS 18:47:36.6100, -02:00:51.100	6	0.370	40.000	Y	N
W43-MM2_3mm	ICRS 18:47:36.6100, -02:00:51.100	3	0.370	80.000	Y	N
W43-MM3_1mm	ICRS 18:47:41.4600, -02:00:27.600	6	0.370	40.000	Y	N
W43-MM3_3mm	ICRS 18:47:41.4600, -02:00:27.600	3	0.370	80.000	Y	N
G337.92_1mm	ICRS 16:41:10.6200, -47:08:02.900	6	0.510	40.000	Y	N
G337.92_3mm	ICRS 16:41:10.6200, -47:08:02.900	3	0.510	80.000	Y	N
G338.93_1mm	ICRS 16:40:34.4200, -45:41:40.600	6	0.510	40.000	Y	N
G338.93_3mm	ICRS 16:40:34.4200, -45:41:40.600	3	0.510	80.000	Y	N
G328.25_1mm	ICRS 15:57:59.6800, -53:58:00.200	6	0.670	40.000	Y	N
G328.25_3mm	ICRS 15:57:59.6800, -53:58:00.200	3	0.670	80.000	Y	N
G327.29_1mm	ICRS 15:53:08.6200, -54:35:30.800	6	0.670	70.000	Y	N
G327.29_3mm	ICRS 15:53:08.6200, -54:35:30.800	3	0.670	80.000	Y	N
W51-IRS2_1mm	ICRS 19:23:39.8100, 14:31:03.500	6	0.370	60.000	Y	N
W51-IRS2_3mm	ICRS 19:23:39.8100, 14:31:03.500	3	0.370	80.000	Y	N
G333.60_1mm	ICRS 16:22:09.3600, -50:05:58.900	6	0.510	80.000	Y	N
G333.60_3mm	ICRS 16:22:09.3600, -50:05:58.900	3	0.510	80.000	Y	N
W43-MM1_3mm	ICRS 18:47:47.0000, -01:54:26.000	3	0.370	80.000	Y	N
G008.67_1mm	ICRS 18:06:19.2600, -21:37:26.700	6	0.670	40.000	Y	N
G008.67_3mm	ICRS 18:06:19.2600, -21:37:26.700	3	0.670	80.000	Y	N
G353.41_1mm	ICRS 17:30:26.2800, -34:41:49.700	6	0.950	80.000	Y	N
G353.41_3mm	ICRS 17:30:26.2800, -34:41:49.700	3	0.950	80.000	Y	N
G010.62_1mm	ICRS 18:10:28.8400, -19:55:48.300	6	0.370	40.000	Y	N
G010.62_3mm	ICRS 18:10:28.8400, -19:55:48.300	3	0.370	80.000	Y	N
G012.80_1mm	ICRS 18:14:13.3700, -17:55:45.200	6	0.950	80.000	Y	N
G012.80_3mm	ICRS 18:14:13.3700, -17:55:45.200	3	0.950	80.000	Y	N
G351.77_1mm	ICRS 17:26:42.6200, -36:09:20.500	6	0.950	80.000	Y	N
G351.77_3mm	ICRS 17:26:42.6200, -36:09:20.500	3	0.950	80.000	Y	N
W51-E_1mm	ICRS 19:23:44.1800, 14:30:29.500	6	0.370	40.000	Y	N

Total # Science Goals : 29

<b>SCHEDULING TIME CONSTRAINTS</b>	NONE	<b>TIME ESTIMATES OVERRIDDEN ?</b>	No
------------------------------------	------	------------------------------------	----

# ALMA-IMF: ALMA transforms our view of the origin of stellar masses

PI F. Motte (EU); co-PI A. Ginsburg (NA); co-PI P. Sanhueza (EA); co-PI F. Louvet (CL)

## 1. Scientific Justification

Thanks to its unmatched angular resolution, sensitivity, image quality, and excellent frequency coverage, ALMA is revolutionizing our understanding of star formation. In previous Cycles, ALMA has imaged in total more than three hundred high-mass star-forming clumps (e.g., projects PI Csengeri; PI Pillai; PI Sanhueza, PI Tan). These observations proved that, generally, the turbulent core model (McKee & Tan 2002) does not apply and that gas inflows play a major role in the (high-mass) star formation process (see review by Motte et al. 2017 and references therein).

**Next breakthrough expected from ALMA is the question of the origin of the initial mass function (IMF).** Recently highlighted by ALMA itself, this question requires a coherent and statistically-meaningful Large Program, ALMA-IMF. It will also provide the community with an unprecedented database with high legacy value for cores, hot cores, stellar clusters, and extragalactic studies. The fine ALMA mosaics resulting from the ALMA-IMF project will broaden our view of high-mass star formation by simultaneously capturing all relevant scales involved in this process, from 1 pc down to 0.01 pc, as well as the concurrent formation of high-mass and low-mass stars.

### 1.1 Scientific rationale: the IMF origin

The number of stars with a given mass at birth, so called IMF, is among the very few key parameters transcending astrophysical fields. It is of paramount importance to current theories ranging from cosmology to stellar physics and exo-planets. The IMF is considered to be universal through virtually all galactic environments studied so far (e.g., Bastian et al. 2010). Its origin, arguably the most central question in star formation, remains a major open issue in modern astrophysics (see review by Offner et al. 2014).

For the past 20 years, both observational surveys and theories of star formation have claimed that stellar masses are determined by cloud fragmentation, and thus by the gas mass of cores (e.g., Motte et al. 1998; Padoan & Nordlund 1999; Chabrier 2003; Könyves et al. 2015). Until today however, observational constraints from so-called core mass functions (CMFs) were limited to regions in our Solar neighborhood, which only form stars with  $0.1 - 5 M_{\odot}$  (e.g., Enoch et al. 2006; André et al. 2014). These regions are unrepresentative of the Galaxy; they do not capture clouds which form stars  $>5M_{\odot}$ , high-mass cloud environments, or our Galaxy in its vast extent and range of conditions. **Our current understanding of the origin of stellar masses is therefore biased if not distorted. Studying massive protoclusters is mandatory to test if the IMF origin can be independent of cloud characteristics.**

### 1.2 Initial studies: CMFs in ‘Young’ to ‘Evolved’ massive protoclusters

Thanks to ALMA, our group has reported on the first definitive observation of a CMF, whose shape is not reminiscent of the IMF (Motte et al. *subm.*, project 2013.1.01365.3S). This CMF comes from W43-MM1, which is a dense cloud efficiently forming stars at the tip of the Galactic bar (Nguyen Luong et al. 2013; Louvet et al. 2014, see **Fig. 1a**). Fitted by a single power-law relation both in the regime of solar-type and high-mass ( $3 - 200 M_{\odot}$  cores), this CMF is flatter than reference

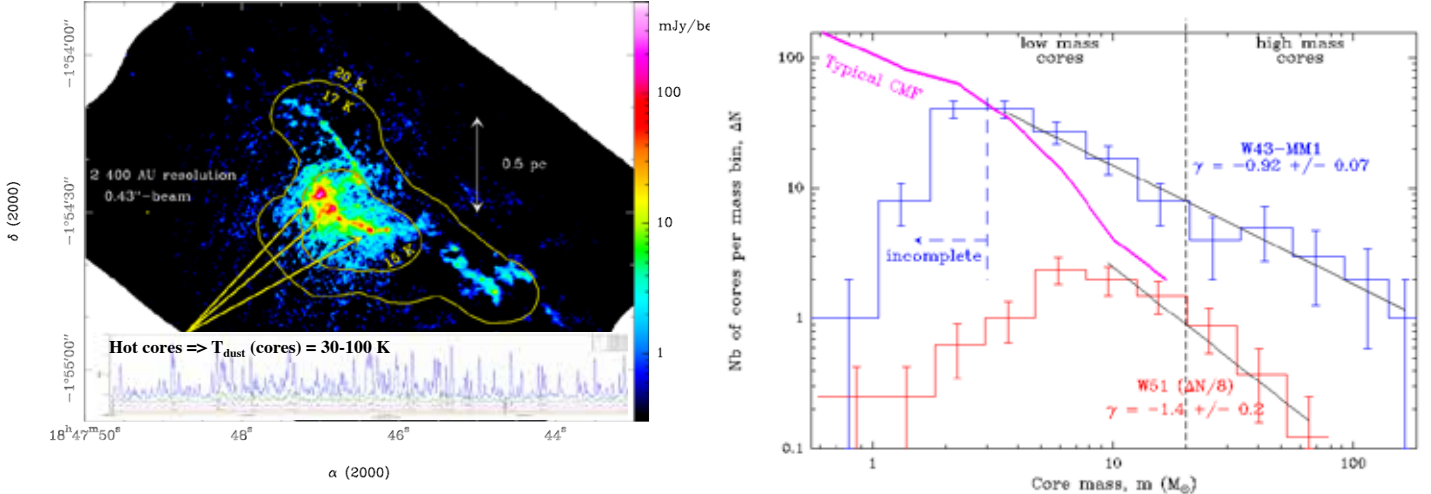


Figure 1: **a)** ALMA 1.3 mm image of the W43-MM1 massive protocluster (color) and our 15-100 K temperature model (contours). Hundreds of 2000 AU cores are extracted in this 2 pc<sup>2</sup> protocluster with a 5 $\sigma$   $\sim$  0.6  $M_{\odot}$  sensitivity. At least 20 cores drive outflows and 6 power hot cores (spectra). **b)** CMF of the W43-MM1 protocluster (blue histogram), fitted by a single power-law,  $dN/d\log(m) \propto m^{\gamma}$  with  $\gamma = -0.92 \pm 0.07$  (red line). It is flatter than the W51 CMF and reference CMF studies in their high-mass range (red histogram and pink curve, Ginsburg et al. in prep.; Könyves et al. 2015).

CMF studies (see **Fig. 1b**). It is also quantitatively flatter than the core mass distribution derived from a one-to-one mapping of the stellar IMF (Salpeter 1955). Such an excess of high-mass cores with respect to their solar-type counterparts has been previously suggested by pointed observations (e.g., Zhang et al. 2015; Csengeri et al. 2017) but could not be substantiated further than a mass segregation effect. For the first time, the large-scale high sensitivity image (several pc<sup>2</sup>, 5 $\sigma$   $\sim$  0.6  $M_{\odot}$ ) of a massive protocluster shows, without any doubts, that low-mass cores with 2000 AU typical sizes are underpopulated at the early stage of protoclusters. Subfragmentation or binarity is unlikely to change the CMF of high-mass cores, whose typical sizes are smaller than that of low-mass (2000 vs. 6000 AU, respectively, Swift & Williams 2008). The atypical CMF of W43-MM1 can be understood if the IMF of massive clusters is not universal but underpopulated with low-mass stars. Alternatively, high-mass stars may only form in dynamical clouds like the young W43-MM1, during the initial cluster formation phase whereas low-mass stars form continuously.

In parallel, our group has imaged the W51 massive protocluster, which is at an evolved stage and whose CMF more closely resembles the IMF shape (Ginsburg et al. 2017, see **Fig. 1b**). **While the IMF may be spatially invariant, these outstanding observations of W43-MM1 and W51 prove that its temporal variability may be the key to understanding the conditions that determine stellar mass.** Massive protoclusters in their first  $\sim 10^5$  years would be underpopulated with low-mass cores and approach the ‘standard’ IMF at later stages, when HII regions have formed at an age of  $\sim 10^6$  yr. These results therefore challenge our current understanding of the IMF origin. Star formation probably is a much more dynamical process than assumed when stipulating that the IMF is simply determined by cloud fragmentation, before the onset of gravitational collapse. **A targeted and in-depth study of a large sample of massive protoclusters is required to determine how young protocluster CMFs evolve both in time and as a function of parent cloud mass. Now is the time for such a focused program; the hard-fought groundwork has been established over the last 20 years, and without this systematic investigation we will have to wait at least another decade, if not more, for the evidence on the origin of stellar masses to emerge in a piecemeal and incoherent fashion.**

## 2. Immediate objectives of the ALMA-IMF Large Program

The ultimate objective of ALMA-IMF is to push forward the understanding of the IMF origin and stimulate improvements to star formation models. To this aim, we will image with ALMA 15 massive protoclusters and apply the robust analysis steps we have identified with our earlier projects.

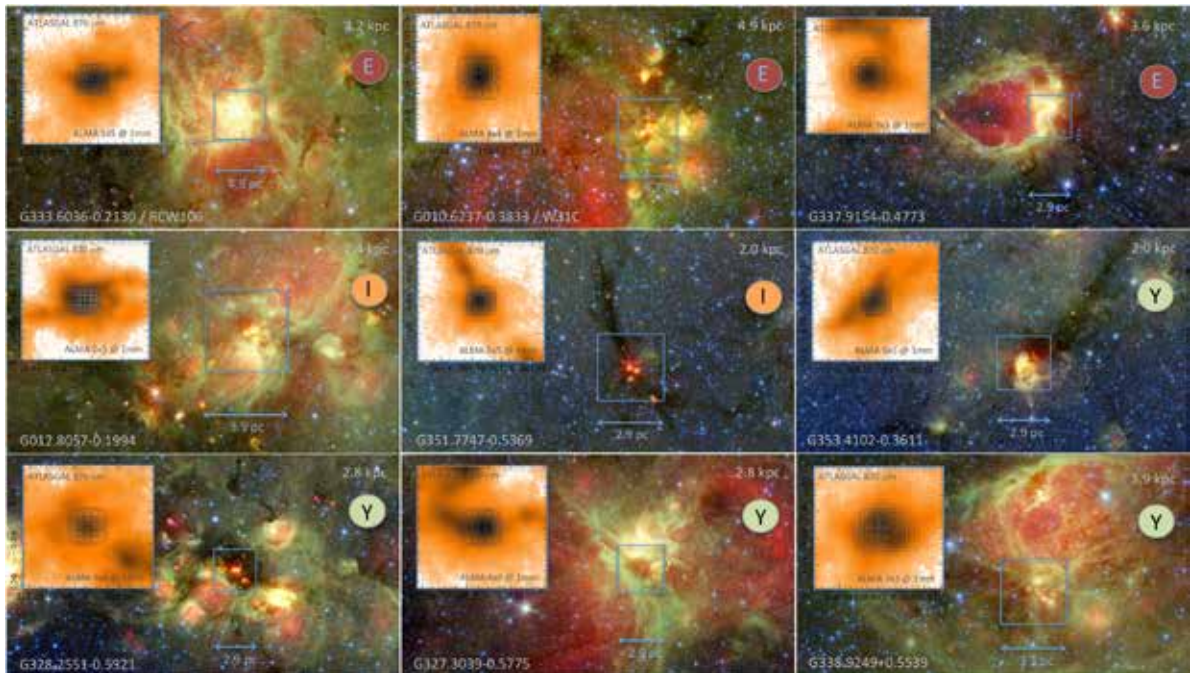


Figure 2: *Nine of the 15 protoclusters we propose to image with ALMA, as seen with Spitzer (3-color). Requested ALMA mosaics are overlaid on the ATLASGAL 870  $\mu\text{m}$  emission (heat color, upper-left panels). Given their  $10^3 - 10^4 M_{\odot}$  masses and the requested sensitivity of  $5\sigma = 0.6 M_{\odot}$ , these 1-2  $\text{pc}^2$  massive protoclusters should host hundreds of 2000 AU cores, with a large mass range.*

### 2.1 Proposed targets: the most massive protoclusters at less than 6 kpc

The APEX/ATLASGAL and CSO/BGPS surveys covered the inner Galactic plane at (sub)millimeter wavelengths, providing uniquely complete samples of sources at 2 to 8 kpc distances (Ginsburg et al. 2013; Csengeri et al. 2014). They revealed particularly massive,  $\text{pc}^2$  protocluster clouds, the best known of which are W43-MM1, W49, W51-IRS2, and Sgr B2. We used the ATLASGAL imaging to perform an unbiased selection of these extreme protoclusters, with  $M(<1\text{pc}^2) = 2 \times 10^3 M_{\odot}$  as mass threshold. While several tens of massive protoclusters were found within the whole Galaxy, a distance-limited criterium of  $d < 6$  kpc provides 15 targets. Further-away protoclusters were excluded to allow studying a large sample of massive protoclusters with reasonable integration times per target. Following evolutionary trends of protostars, the luminosity-to-mass ratio provides a fair evolutionary indicator for  $\sim\text{pc}^2$  protoclusters, which we qualify as ‘Young’ when  $L/M < 25 L_{\odot}/M_{\odot}$ , ‘Intermediate’ when  $L/M \sim 25 - 50 L_{\odot}/M_{\odot}$ , and ‘Evolved’ for  $L/M > 50 L_{\odot}/M_{\odot}$ . Among basic image parameters, the carefully-defined mosaics are shown in **Fig. 2** and given in **Table 1**.

The ALMA-IMF Large Program targets a nearby, complete sample of massive protoclusters at 2–6 kpc. Thanks to its high sensitivity and angular resolution, ALMA-IMF will reveal one thousand cores, 8 times more than found in W43-MM1 alone, above the CMF peak at  $\sim 0.6 M_{\odot}$ . **Table 1** sample is necessary and sufficient to differentiate between CMF and IMF slopes, as

well as to follow CMFs from the ‘Young’ to the Evolved’ stage of massive protoclusters (compare curves in Fig. 1b). Lying within mini-starburst complexes of the Milky Way, these massive protoclusters span a large LST range (11h–22h). It thus keeps the fraction of observing time per configuration and LST in ALMA-IMF within Large Program time constraint limits.

Table 1: Complete sample of massive protoclusters at  $<6$  kpc, of various evolutionary stages

Name	d [kpc]	$M(<pc^2)$ [ $M_{\odot}$ ]	$L_{bol}/M$ [ $L_{\odot}/M_{\odot}$ ]	Mosaic, Resol [" $\times$ ", " $''$ ]	$1\sigma$ 1/3mm [ $\mu$ Jy/beam]	Req. time 1mm+3mm	Resp. region
<b>Young protoclusters</b>							
G030.82=W43-MM1	5.5	$16 \times 10^3$	3.9	$120 \times 80$ , 0.37	–/30	0 + 5.3 hr	EU
G338.93	3.9	$8.0 \times 10^3$	9.3	$55 \times 55$ , 0.51	200/60	1 + 1.2 hr	EA
G327.29	2.8	$6.5 \times 10^3$	10	$70 \times 70$ , 0.67	300/90	0.6 + 0.7 hr	EA
G030.70=W43-MM2	5.5	$13 \times 10^3$	11	$60 \times 60$ , 0.37	100/30	3.1 + 5.3 hr	CL
G328.25	2.8	$4.2 \times 10^3$	13	$70 \times 70$ , 0.67	300/90	0.6 + 0.7 hr	EU
G353.41	2.0	$3.3 \times 10^3$	13	$100 \times 100$ , 0.95	600/180	0.6 + 0.7 hr	NA
G008.67	3.4	$2.7 \times 10^3$	16	$70 \times 70$ , 0.67	300/90	0.6 + 0.7 hr	EA
<b>Intermed protoclusters</b>							
G049.49M=W51-E	5.4	$22 \times 10^3$	25	$60 \times 60$ , 0.37	100/30	3.6 + 4.1 hr	NA
G351.77	2.0	$2.2 \times 10^3$	29	$100 \times 100$ , 0.95	600/180	0.6 + 0.7 hr	EU
G030.72=W43-MM3	5.5	$6.6 \times 10^3$	30	$60 \times 60$ , 0.37	100/30	3.2 + 5.3 hr	EU
G012.80=W33	2.4	$5.2 \times 10^3$	46	$100 \times 100$ , 0.95	600/180	0.6 + 0.7 hr	CL
<b>Evolved protoclusters</b>							
G337.92	3.6	$3.0 \times 10^3$	50	$55 \times 55$ , 0.51	200/60	1.0 + 1.2 hr	EA
G010.62=W31C	4.9	$7.4 \times 10^3$	54	$60 \times 60$ , 0.37	100/30	4.7 + 3.4 hr	NA
G049.49=W51-IRS2	5.4	$14 \times 10^3$	69	$60 \times 60$ , 0.37	100/30	3.7 + 4.1 hr	NA
G333.60	4.2	$13 \times 10^3$	130	$110 \times 110$ , 0.51	200/60	3.2 + 1.9 hr	CL

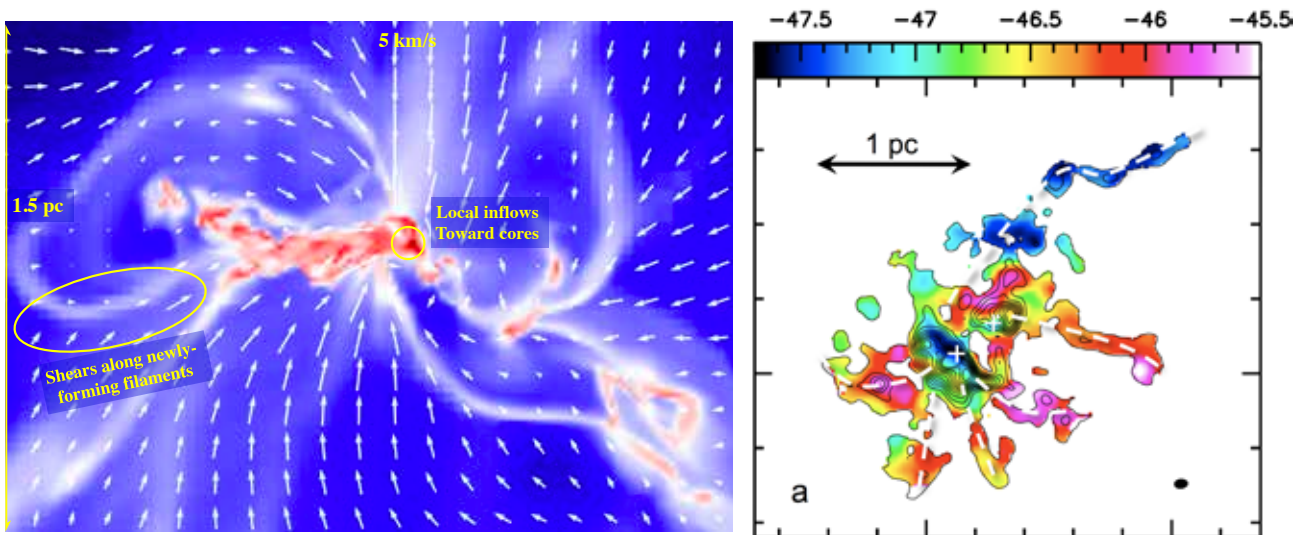


Figure 3: a) Gas flows observed to converge toward a protocluster, in MHD numerical simulations by Lee & Hennebelle (2016). At center, cores are locally fed by small-scale inflows while new filaments form in the surrounding. b) Gas flows observed by ALMA toward a high-mass star formation clump, from  $2 \text{ km s}^{-1}$  velocity drifts of dense gaz traced by the  $\text{N}_2\text{H}^+(1-0)$  line (Peretto et al. 2013).

## 2.2 Analysis steps of the ALMA-IMF Large Program

The ALMA-IMF Large Program aims to follow the evolution in time of the CMF/IMF relationship in massive protoclusters and explain it through the quantification of gas inflows toward and outflows

from detected cores. To resolve the  $\sim 2000$  AU typical diameter of cores (Bontemps et al. 2010; Palau et al. 2013) and image the  $\sim 1\text{--}2$  pc<sup>2</sup> protocluster extent, we will make 1 mm and 3 mm mosaics (extents in **Table 1**) with  $0.4'' - 1''$  synthesized beams depending on the distance. We chose **1 mm and 3 mm spectral bands** primarily for their mostly optically thin emission in massive cores and their well-defined dust emissivity ( $\kappa_{1\text{mm}} = 0.01 \text{ cm}^2 \text{ g}^{-1}$  and  $\kappa_{3\text{mm}} = 0.003 \text{ cm}^2 \text{ g}^{-1}$ ). The chosen setups cover, among the main lines, **<sup>12</sup>CO(2-1) and N<sub>2</sub>H<sup>+</sup>(1-0)** to measure gas mass outflows and inflows, **<sup>13</sup>CS and N<sub>2</sub>D<sup>+</sup>** to estimate core turbulence levels, the **H41 $\alpha$**  recombination line to identify HII regions, and **CH<sub>3</sub>OH, CH<sub>3</sub>CN, and CH<sub>3</sub>CCH** to probe gas temperature. Combining ALMA with ACA (+TP) is necessary for a proper analysis of outflows and inflows. For each protocluster, we will follow an analysis strategy in five steps, defined for the W43-MM1 project:

1. **Core identification in ALMA images (WG1 & WG2):** We will reduce data following the strategy of our past Cycle projects, aiming to minimize interferometric artefacts while keeping low-mass cores: most sensitive self-calibration, combination with ACA and multi-scale cleaning. We will then extract cores with Getsources (Men'shchikov et al. 2012), simultaneously on the full and line-free continuum bands for detecting both low-mass and hot core sources. Several runs will be done to determine the robustness of the extracted CMF shape and its completeness level, limited at mosaic center by ALMA dynamical range (e.g. **Fig. 1a**).
2. **Core nature and massive protocluster evolutionary stage (WG3):** The pre-stellar, protostellar, or HII region nature of cores will be investigated through outflows imaged in CO, SiO, and SO lines, through hot cores traced by complex organic molecules (see **Fig. 1a**), and through H41 $\alpha$  recombination line. The evolutionary stage of protoclusters will be estimated from the typical age of its massive cores:  $10^6$  yr for HII regions and  $10^5$  yr for protostars.
3. **Core mass determination (WG4):** A good mass determination is a pre-requisite for a proper CMF. We will use 1 mm fluxes in the first place but 3 mm fluxes when the former is optically thick. Fluxes will be corrected for line or free-free contaminations, using line-free bands and radio (archival and GLOSTAR project from Menten) plus ALMA 3 mm fluxes. We will build dust temperature models dedicated to cores using the combination of 1) a Bayesian SED fitting method applied to all existing continuum images including ALMA (PPMAP; Marsh et al. 2015) and 2) hot core temperatures measured through line excitation temperatures of complex organic molecules found in all bands (see **Fig. 1a**).
4. **CMF evolution (WG5 & WG9):** CMFs of prestellar (and IR-quiet protostellar) cores will be compared with IMF models of binaries/systems (Hopkins 2013; Hennebelle & Chabrier 2013), CMFs derived in low-mass star-forming clouds (e.g., Könyves et al. 2015) and extragalactic environments (e.g., project PI Braine). Our requested sensitivities (see **Table 1**) will allow a  $5\sigma$  detection of cores down to the CMF peak,  $0.6 M_{\odot}$  when assuming  $T_{\text{dust}} = 20$  K. **For ‘Young’ massive protoclusters, we will use the much larger statistics (8 $\times$ ) of ALMA-IMF to definitively determine whether the low-mass part of their CMFs is flatter than the IMF.** CMF evolution through protocluster age will also be investigated by averaging the CMF of ‘Young’, ‘Intermediate’, and ‘Evolved’ massive protoclusters.
5. **Core mass evolution, new core formation events (WGs 6–8):** Local inflowing gas streams toward individual cores traced by N<sub>2</sub>H<sup>+</sup> (see **Figs. 3a-b**, e.g., Csengeri et al. 2011, Peretto et al. 2013) will be quantified to check if gas feeding can explain a CMF that reconciles the IMF shape at late stages. Outflowing gas mass will also be measured by <sup>12</sup>CO line wings to estimate the mechanical feedback of outflows as proposed by Matzner & McKee (2000). CMF models, which tried to account for core mass growth or magnetic field effect on filament

fragmentation (e.g., Hatchell & Fuller 2008; Smith et al. 2008; Lee & Hennebelle in prep.) will be improved with our kinematical and CMF constraints. The formation of a new generation of filaments and cores traced by large-scale inflows and SiO shocks (see **Fig. 3a**, e.g., Sanhueza et al. 2013, Louvet et al. 2016) will also be used to determine if it can be the main process behind the CMF evolution.

### 3. Management plan and Data products

The ALMA-IMF Large Program is backed by a consortium of 30 people, organized in analysis working groups constituted by world-class experts and including two PhD students (see **Table 2**). The CMF publications of individual massive protocluster will be shared between each region. Communication will be ensured and collaboration will be favored by monthly telecons, yearly meetings and a twiki.

Each region will share the responsibility to process the ALMA-IMF data with common CASA scripts and Getsources input parameters, on their local ALMA data processing infrastructures (e.g., the new 140 Tb computer facility at OSUG Grenoble). Fully-reduced (calibrated, combined with ACA data, and cleaned) bands and major line datacubes will be distributed, along with associated scripts through ARC nodes, to the community after 12 months of the raw data delivery. As soon as papers are published the consortium will undertake to provide several value-added products via the website of the EU funded COMPET 2015 StarFormMapper: 1) complete core catalogs with their size, flux, dust temperature, mass, and density, 2) temperature map models derived from from PPMAP and hot core informations, and 3) 1 mm and 3 mm spectral bands toward individual cores.

Table 2: *Working Groups of the ALMA-IMF Large Program*

Working group & Task	Main Participants
WG0 : Large Program management	Motte/Csengeri, Ginsburg, Sanhueza, & Louvet
WG1: Data reduction	Galván-Madrid, Lopez-Sepulcre, Louvet, Sanhueza
WG2: Core extraction	Bontemps, Ladjelate, Louvet, Motte, Ohashi, Rosolowky
WG3: Core nature (outflows, H IIs)	Csengeri, Galván-Madrid, Ginsburg, Menten, Sakai
WG4: Dust temperature, hot cores	Chen, Guzmán, Herpin, Lu, Marsh, Molet(PhD)
WG5: CMF comp. w. low-mass or Xgal	Braine, Di Francesco, Nakamura, Ohashi, Stutz
WP6: Core mass growth by inflow	Battersby, Csengeri, Louvet, Lu, Nony, Svoboda
WP7: Core mass decrease by outflow	Bally, Bontemps, Bronfman, Nakamura, Nony(PhD)
WP8: Building up of new filaments	Bronfman, Gusdorf, Louvet, Nguyen Luong, Sanhueza
WP9: CMF comparison with models	Hennebelle, Gomez, Ginsburg, Louvet, Motte, Sanhueza

**References:** • André et al. 2014, *Protostars and Planets VI*, 27 • Bastian et al. 2010, *ARA&A*, 48, 339 • Bontemps et al. 2010, *A&A*, 524, 18 • Chabrier 2003, *PASP*, 115, 763 • Csengeri et al. 2011, *ApJL*, 740, L5 • Csengeri et al. 2014, *A&A*, 565, 75 • Csengeri et al. 2017, *A&A*, in press • Enoch et al. 2006, *ApJ*, 638, 293 • Ginsburg et al. 2013, *ApJS*, 208, 14 • Ginsburg et al. 2017, *ApJ*, in press • Hatchell & Fuller 2008, *A&A*, 482, 855 • Hennebelle & Chabrier 2013, *ApJ*, 770, 150 • Hopkins 2013, *MNRAS*, 433, 170 • Könyves et al. 2015, *A&A*, 584, 91 • Lee & Hennebelle 2016, *A&A*, 591, 30 • Louvet et al. 2014, *A&A*, 570, 15 • Louvet et al. 2016, *A&A*, 595, 122 • Marsh et al. 2015, *MNRAS*, 454, 4282 • McKee & Tan 2002, *Nature* 416, 59 • Men'shchikov et al. 2012, *A&A*, 542, 81 • Motte et al. 1998, *A&A*, 336, 150 • Motte et al. 2017, *ARA&A*, 55, in press • Motte et al. *subm. to Nature Astronomy* • Nguyen Luong et al. 2013, *ApJ*, 775, 88 • Offner et al. 2014, *Protostars and Planets VI*, 53 • Padoan & Nordlund 1999, *ApJ*, 526, 279 • Palau et al. 2013, *ApJ*, 762, 120 • Peretto et al. 2013, *A&A*, 555, 112 • Salpeter 1955, *ApJ*, 121, 161 • Sanhueza et al. 2013, *ApJ*, 773, 123 • Smith et al. 2008, *MNRAS*, 391, 109 • Swift & Williams 2008, *ApJ*, 679, 552 • Zhang et al. 2015, *ApJ*, 804, 141